ISSN 0208-7774 TRIBOLOGIA 4/2017 p. 139–147

Wojciech ŻÓRAWSKI[*], Medard MAKRENEK[**], Anna GÓRAL[***], Sławomir ZIMOWSKI[****]

HVOF SPRAYED NANOSTRUCTURED COMPOSITE COATINGS WITH A REDUCED FRICTION COEFFICIENT

PŁOMIENIOWO NATRYSKANE NADDŹWIĘKOWO NANOSTRUKTURALNE POWŁOKI KOMPOZYTOWE Z OBNIŻONYM WSPÓŁCZYNNIKIEM TARCIA

Key words: solid lubricant, composite coating, HVOF.

Abstract Nanostructured materials provide new possibilities, which enable creating composite structures with much better properties than composites obtained from conventional materials. Such a solution facilitates combining selected features of different nanomaterials in order to obtain a composite with the required durability, thermal, insulation, tribological, etc. properties. In the case of a composite containing a solid lubricant, it is comprised of a nanostructured matrix, providing mechanical durability, and an evenly distributed nanostructured solid lubricant. A study of the tribological properties of composite HVOF sprayed from nanostructured WC-12Co mixed with nanostructured Fe_3O_4, having the properties of the solid lubricant is presented. The coatings were sprayed by means of a Hybrid Diamond Jet system. A T-01 ball on disc tribological tester was used to determine the coefficient of friction on the basis of friction force obtained in the course of continuous measurement at a set load. The result of investigations was compared with properties of coatings sprayed with standard WC-12Co/ Fe_3O_4.

Słowa kluczowe: smar stały, powłoka kompozytowa, płomieniowe natryskiwanie naddźwiękowe.

Streszczenie Materiały nanostrukturalne stwarzają nowe możliwości, które pozwalają na tworzenie struktur kompozytowych o właściwościach znacznie lepszych niż te otrzymywane z materiałów konwencjonalnych. Takie rozwiązanie umożliwia łączenie wybranych właściwości różnych nanomateriałów w celu uzyskania kompozytu, który będzie posiadał wymagane właściwości wytrzymałościowe, tribologiczne, cieplne i inne. W przypadku kompozytów zawierających smar stały składają się one z nanostrukturalnej matrycy zapewniającej wytrzymałość mechaniczną i równomiernie rozłożonego nanostrukturalnego smaru stałego. W artykule przedstawiono badania właściwości tribologicznych płomieniowo natryskanego naddźwiękowo kompozytu będącego mieszaniną nanostrukturalnego proszku WC-12Co i nanostrukturalnego proszku Fe_3O_4 o właściwościach smaru stałego. Powłoki kompozytowe zostały natryskane z użyciem systemu do płomieniowego natryskiwania naddźwiękowego Hybrid Diamond Jet. Tester tribologiczny T-01 typu kulka-pierścień został użyty do zbadania współczynnika tarcia na podstawie pomiaru siły tarcia otrzymanej w wyniku ciągłego pomiaru przy ustalonym obciążeniu. Wyniki badań zostały porównane z właściwościami powłok płomieniowo natryskanymi naddźwiękowo z konwencjonalnych proszków WC-12Co/Fe_3O_4.

INTRODUCTION

Friction and wear issues are constantly up-to-date in all industries, because they are crucial to its effectiveness. Properly constructed friction nodes should have high wear resistance, which allows for considerable material savings and low friction coefficient, which in turn reduces the amount of energy consumed to overcome the drag resistance. Compliance with these requirements is made possible by the appropriate selection of materials for the steam and the introduction of a lubricant that is delivered to areas where friction occurs. The lack of direct contact with the surface of the vacuum couple allows the elimination of pathological wear processes such as wear, abrasion, and heat wear. The separation of these surfaces can be achieved by means of liquid or plastic lubricants. This, however, requires the introduction of a suitable lubrication system with seals

[*] Kielce University of Technology, Laser Research Processing Centre, ul. Tysiąclecia Państwa Polskiego 7, 25-314 Kielce, Poland.
[**] Kielce University of Technology, Faculty of Management and Computer Modelling, ul. Tysiąclecia Państwa Polskiego 7, 25-314 Kielce, Poland.
[***] Institute of Metallurgy and Materials Science PAS, Cracow, ul. Reymonta 25, 30-059 Kraków, Poland.
[****] AGH University of Science and Technology, Faculty of Mechanical Engineering and Robotics, ul. A. Mickiewicza 30, 30-059 Kraków, Poland.

and heat exchangers. Service is also needed to control the quantity and quality and to replenish the required amount of lubricant. In the event of a malfunction of the lubrication system, there is an accelerated wear and then a malfunction **[L. 1–3]**.

Thermal spraying techniques provide a wide range of possibilities of applying solid lubricants onto the surfaces of mating machine elements **[L. 4–8]** and the application of the coating material with a solid lubricant for spraying results in obtaining a thin film. It can be coated onto a given element that can operate in a wide range of conditions. Utilising molybdenum disulphide in the process of thermal spraying allows considerably improving the operating conditions of the interacting elements. Taking into consideration high temperatures present in the spray stream, molybdenum disulphide can be subject to decomposition, thus additionally forming MoO_3. Its presence in the friction area is unfavourable due to its hardness. Despite the fact that heat resistance molybdenum disulphide in the air reaches 500°C, the maximum operating temperature should not exceed 400°C; however, in the vacuum, it retains its properties at 700°C **[L. 9–11]**. A thin nickel coating is used to protect it against harmful effects of temperature. A composite coating obtained by detonation spraying of WC-12Co powder with a 10% addition of MoS_2-Ni exhibited a lower coefficient of friction and wear **[L. 12]**. The necessity to protect molybdenum disulphide against the high temperature of the spraying stream results from its high melting temperature, i.e. 1185°C. In the case of spraying it in a mixture with WC-Co, its temperature is 307°C lower than the melting temperature of cobalt, i.e. 1492°C. Powder grain should reach ca. 2000°C during detonation spraying, which guarantees the best resistance properties of WC-Co coating. Unfortunately, this temperature causes complete melting of MoS_2 grains, which are subject to decomposition and are not deposited on the substrate. Only lowering the spraying stream temperature enables one to obtain a coating with molybdenum disulphide **[L. 11]**. Preparing composite powder is more expensive and technologically complex; nevertheless, it facilitates avoiding solid lubricant degradation and improves coating properties. A mixture of WC-12Co powders, copper, and molybdenum disulphide underwent sintering and then crushing. The plasma sprayed coating contained both Cu and MoS_2, and, in addition, the occurrence of copper contributed to considerable lowering the level of tungsten carbide decomposition. As a consequence, the WC-12Co/Cu/MoS_2 coating had not only a lower coefficient of friction but also an increased wear resistance compared to WC-12Co **[L. 13]**.

Iron oxides are currently a component of many composite coatings in which they are responsible for their tribological properties. For plasma-sprayed and PTWA-sprayed coatings on the surfaces of cylinders of combustion car engines, in the conditions of heavy loads and high temperatures, oxides FeO and Fe_3O_4 play a fundamental role in friction processes. The presence of Fe_2O_3 in the coating considerably increases resistance to wear **[L. 14, 15]**. Composite materials for spraying containing iron oxides in their composition have been used in numerous applications for many years. It is recommended to apply a mixture of 40% of Cr_3C_2 and 60% of Fe_3O_4 for one of the solutions for the plasma spraying of piston rings and cylinder liners **[L. 16]**.

This work presents results concerning the nanostructured composite coatings containing a nanostructured solid lubricant. The coatings were made by mixing the powders of WC-12Co, which assures very high wear resistance, and Fe_3O_4, which exhibits the properties of a solid lubricant.

METHODOLOGY

In the present study, nanostructured and conventional tungsten carbide powders were applied as the matrix in WC-12Co/Fe_3O_4 composite coatings. Nanostructured WC12-Co powder was Nanox™S7412 produced by Inframat Advanced Materials (IAM). Amperit 519.074 WC-12Co powder was used as the matrix in conventional composite coatings. Iron (II, III) oxide, Fe_3O_4, was applied as a solid lubricant. As the crystalline structure suggests and the literature data **[L. 17, 18]** confirm, we can assume that the properties of Fe_3O_4 as a solid lubricant are appropriate. Nanostructured IAM Nanox™26FE23 Fe_3O_4 powder and conventional IAM Inflox™26FE23 Fe_3O_4 powder were applied to produce WC-12Co/Fe_3O_4 nanostructured and conventional composite coatings, respectively. The composite coatings were sprayed from a mixture of the conventional powders (Amperit 519.074 90%WC12Co + Inflox™26FE23 10%Fe_3O_4) and a mixture of the nanostructured powders (NanoxS7412 90% WC-12Co + Nanox™26FE23 10%Fe_3O_4). The weighed components were mixed in a V-blender for 1 hour prior to spraying. For the metallographic examination, the coatings were deposited on thin flat samples of low-carbon steel with dimensions of 30 mm x 30 mm x 3 mm; whereas, for the tribological tests the coatings were deposited on ring-shaped low-carbon steel samples with dimensions of ϕ46 mm x ϕ25 mm x 6 mm. Before the spraying, the substrate was degreased and grit blasted with electrocorundum EB-12 at a pressure of 0.5 MPa. The thickness of the coatings after spraying was 0.3 – 0,4 mm. The High Velocity Flame Spraying (HVOF) process was performed by means of Sulzer Metco Hybrid Diamond Jet. A mixture of propane and oxygen was used as a fuel. The employed spraying parameters were a propane pressure of 0.69 MPa, a propane flow rate of 77 Nl/min, an oxygen pressure of 1.03 MPa, an oxygen flow rate of 253 Nl/min, an air pressure of 0.72 MPa, an air flow

rate of 336 Nl/min, a carrier gas of argon, and a spray distance of 180 mm.

The structure and chemical composition of the powders and coatings were analysed using scanning microscopes: JSM–5400 equipped with an ISIS 300 Oxford (EDS) microprobe and FEI Nova™ NanoSEM 200.

A T-01 M ball-on-ring tribo-tester was used to determine the coefficient of friction for the HVOF sprayed coatings. The diameter of the 100Cr6 bearing steel ball was 0.635 mm (¼''). The ring-shaped samples were sprayed and subsequently ground as well as polished for one hour. The tests required registering and controlling the action of the friction force in the function of time. The parameters for the T-01M tester were as follows: load – P = 4.9 N, linear velocity – v = 0.5 m/s, and test duration – t = 1 h.

RESULTS AND DISCUSSION

Powders

The properties of the sprayed coatings were dependent not only on the spraying parameters but also on the morphology of the powder particles and the powder phase composition, with the latter being particularly important for nanostructured powders.

The shape of the particles of the Amperit 519.074 WC-12Co powder is presented in **Fig. 1a**. The almost spherical shape of the particles is characteristic of powders produced by agglomeration and sintering. Part of the powder particles is porous. They differ in size, but there are a large number of very fine particles.

The powder producer specifies that a single particle is made up of tungsten carbide particles 1 μm in size, which can be seen in the surface image (**Fig. 2a**). The particles of the Nanox WC-12Co powder (**Fig. 1b**) have an irregular shape. Some of them are spherical. The producer of the nanostructured powder specifies that a single particle is made up of tungsten carbide particles ranging from 100 to 500 nm in size. Using the results of the particle surface analysis (**Fig. 2b**), one can conclude that the particles are finer than those of the conventional WC-12Co powder, especially if the comparison is based on the particle surface morphologies (**Fig. 2a**). The particles ranging from 100 to 500 nm in size are visible on the surface of the powder particle only if higher magnifications are used (**Fig. 3**). The particles of the Inflox™26FE23 Fe_3O_4 powder are shown in **Fig. 1c**. Some of them have a regular spherical shape, which is characteristic of the powders obtained by agglomeration and sintering (**Fig. 1c**). Part of these spherical particles are cracked or otherwise damaged. There are many very fine flakes, which tend to adhere to the larger spherical particles. The surface analysis of the spherical particles (**Fig. 2c**) shows that they are made up of very fine Fe_3O_4 particles with pores in between. Particles of the Nanox™26FE23 Fe_3O_4 powder are shown in **Fig. 1d**. Some of them have an irregular spherical shape, smaller particles are also visible. The surface analysis (**Fig. 2d**) indicates that the powder particle is highly porous and grains of particles consist of submicron particles (**Fig. 2d**).

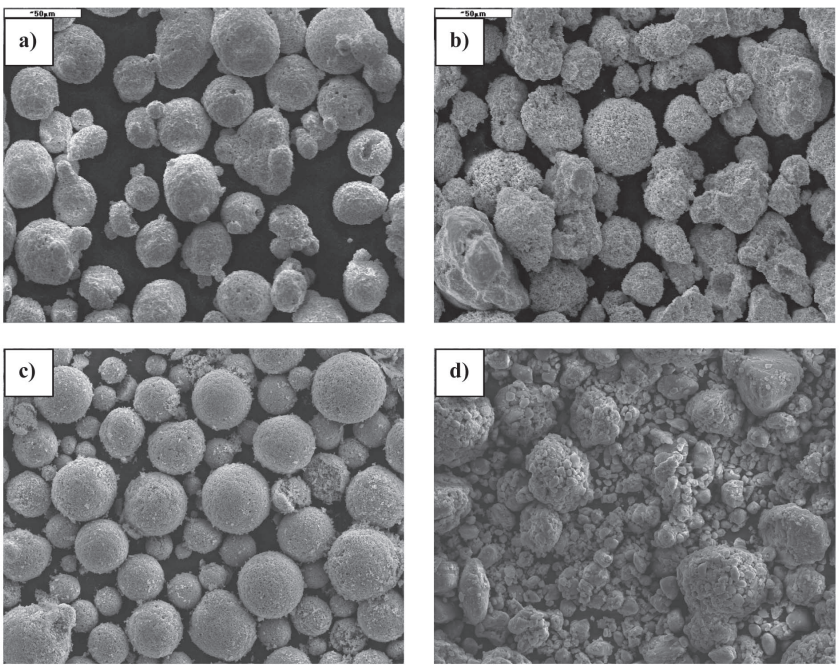

Fig. 1. Powder particle morphology: a) Amperit 519.074 WC-12Co, b) Nanox™S7412 WC-12Co, c) Inflox™26FE23 Fe_3O_4, d) Nanox™26FE23 Fe_3O_4

Rys. 1. Morfologia cząstek proszku: a) Amperit 519.074 WC-12Co, b) Nanox™S7412 WC-12Co, c) Inflox™26FE23 Fe_3O_4, d) Nanox™26FE23 Fe_3O_4

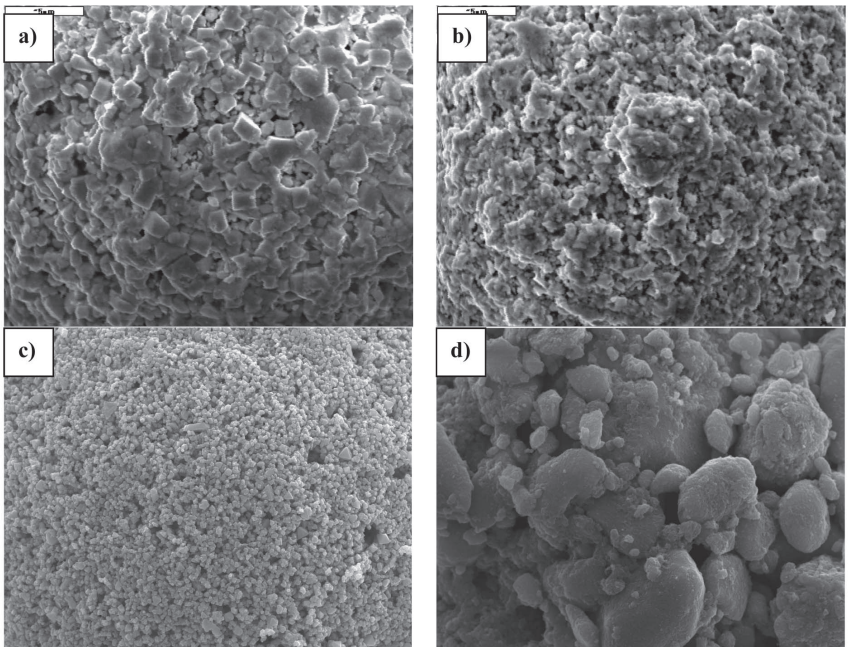

Fig. 2. Surface morphology of powder grain: a) Amperit 519.074 WC-12Co, b) Nanox™S7412 WC-12Co, c) Inflox™26FE23 Fe_3O_4, d) Nanox™26FE23 Fe_3O_4

Rys. 2. Morfologia powierzchni ziarna proszku: a) Amperit 519.074 WC-12Co, b) Nanox™S7412 WC-12Co, c) Inflox™26FE23 Fe_3O_4, d) Nanox™26FE23 Fe_3O_4

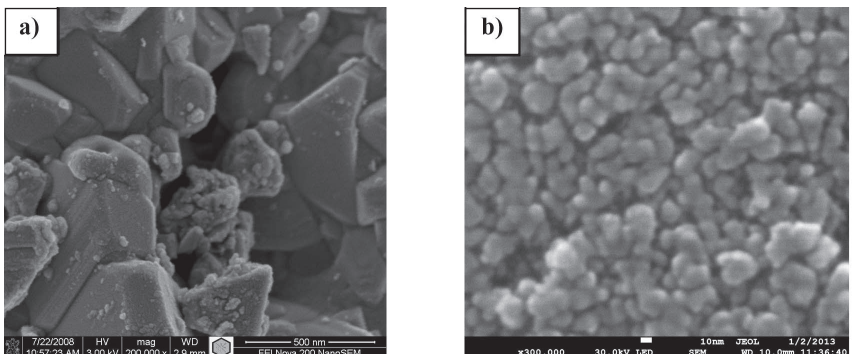

Fig. 3. Particle surface morphology of nanostructured powder at high magnification: a) WC-12Co Nanox™S7412, b) Fe_3O_4 Nanox™26FE23

Rys. 3. Morfologia powierzchni ziarna proszku nanostrukturalnego przy dużym powiększeniu: a) WC-12Co Nanox™S7412, b) Fe_3O_4 Nanox™26FE23

Figure 4 shows the particle size distribution and the relative particle density distribution determined by means of a Sympatec Gmbh Helios laser analyser. The curves plotted for the Amperit WC-12Co powder (**Fig. 4a**) indicate that it has a narrow particle size range (18–55 μm) and can be used for thermal spraying (d_{10} = = 21.59 μm, d_{50} = 31.68 μm, d_{90} = 43.37 μm). The tangent of the inclination of the cumulative distribution curve, n, is 4.07. The Nanox S7412 WC-12Co powder (**Fig. 4b**) has a particle size range of 21–103 μm, which makes it suitable for thermal spraying; however, the participation of large grains is not advantageous. The range, however, is wider than that of the Amperit WC-12Co powder (d_{10} = 22.70 μm, d_{50} = 34.52 μm, d_{90} = 61.28 μm). The tangent of the inclination of the cumulative distribution curve, n, is smaller – 2.33. The curve plotted for the Inflox™26FE23 Fe_3O_4 powder (**Fig. 4c**) illustrates that it has a very wide particle size range. The tangent of the inclination of the cumulative distribution curve, n, is 0.16. The particle sizes range from 0.9 μm up to 175 μm (d_{10} = 0.69 μm, d_{50} = 17.47 μm, d_{90} = 164.38 μm). Particles smaller than 0.9 μm constitute as much as 21.09%. The curves obtained for the Nanox™26FE23 Fe_3O_4 powder (**Fig. 4d**) show that, like in the previous case, the powder has a very wide particle size range and a large content of fine particles. The tangent of the inclination of the cumulative distribution curve, n, is 1.05 (d_{10} = 1.08 μm, d_{50} = 5.95 μm, d_{90} = 17.41 μm).

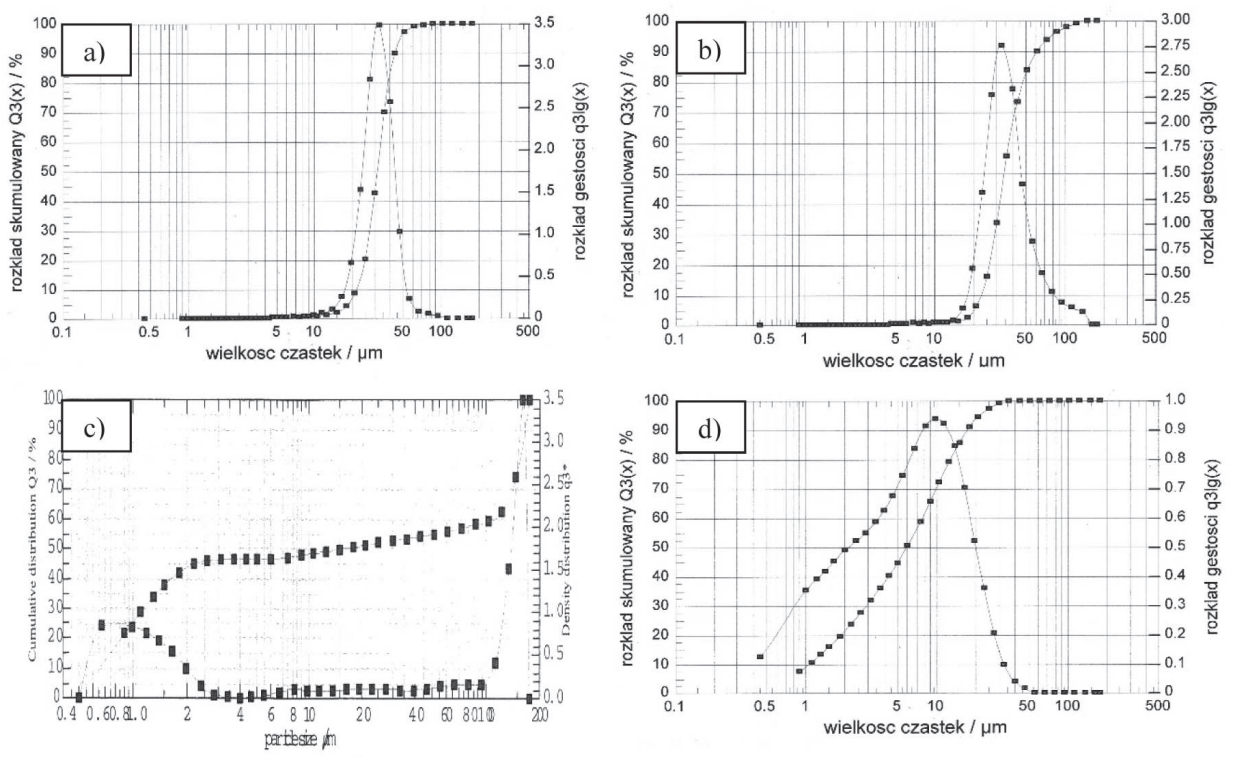

Fig. 4. Particle size distribution for: a) the Amperit 519.074 WC-12Co powder, b) the Nanox™S7412 WC-12Co powder, c) the Inflox™26FE23 Fe_3O_4 powder, d) the Nanox™26FE23 Fe_3O_4 powder

Rys. 4. Rozkład granulometryczny proszku: a) the Amperit 519.074 WC-12Co powder, b) the Nanox™S7412 WC-12Co powder, c) the Inflox26FE23 Fe_3O_4 powder, d) the Nanox™26FE23 Fe_3O_4 powder

Coatings

The metallographic images of two WC-12Co coatings (**Fig. 5**) show that there are some small undeformed tungsten carbide grains embedded in the cobalt matrix. From the EDS microanalysis, it is clear that the coating composition is different in each zone. The light-coloured grains in the WC-12Co coatings testify to a high amount of tungsten; whereas, the dark-coloured matrix is an area with a high content of cobalt and a low content of tungsten. The different sizes of tungsten carbide grains are visible in both coatings. The coating deposited using the nanostructured powder has a more fine-grained structure with unmodified nanocrystals. It exhibits lower porosity, despite the fact that the nanostructured powder contained bigger grains. The coating produced from the conventional powder, on the other hand, has the higher porosity resulting from the higher porosity of the grains, which is seen in the metallographic images. The microstructure of two WC grains in Nanox™S7412 WC-12Co coating and diffraction pattern (SADP) is presented in **Fig. 6**. The grains are surrounded by an amorphous cobalt matrix. The range of grains dimensions is 200–500 µm. SADP corresponds with WC hexagonal orientation **[L. 12]**.

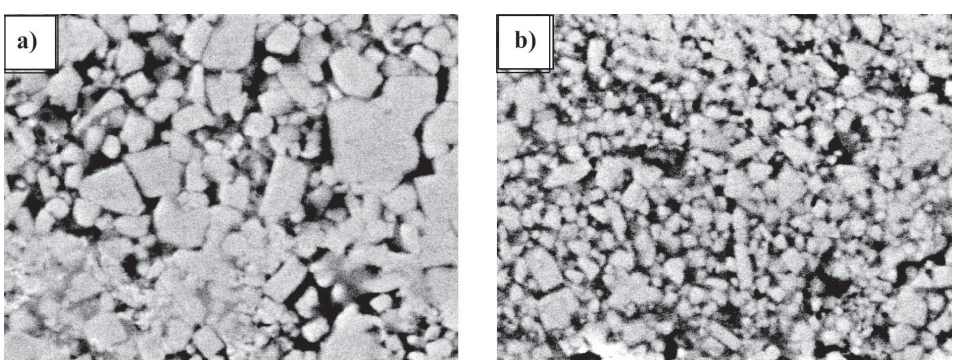

Fig. 5. Cross-section of HVOF sprayed coating: a) Amperit 519.074 WC-12Co, b) Nanox™S7412 WC-12Co

Rys. 5. Zgład metalograficzny płomieniowo natryskanej naddźwiękowo powłoki: a) Amperit 519.074 WC-12Co, b) Nanox™S7412 WC-12Co

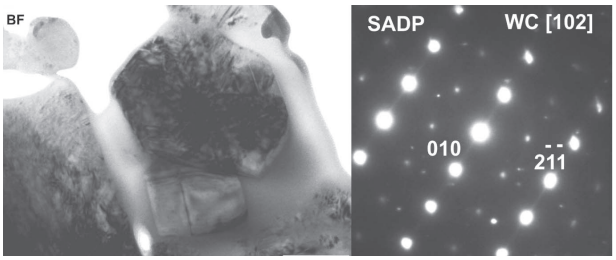

Fig. 6. WC grains in Nanox™S7412 WC-12Co coating
Rys. 6. Ziarna WC w powłoce Nanox™S7412 WC-12Co

Figure 7a shows the microstructure of the HVOF sprayed Inflox Fe_3O_4 coating. There are clear boundaries between the slightly deformed powder particles and the pores. Despite the fact that iron (II, III) oxide has a higher melting point and it is mainly used for plasma spraying, it is also suitable for the high velocity oxy-fuel process, where it forms a coherent coating with visible small pores. The microstructure of the HVOF sprayed Nanox Fe_3O_4 coating is illustrated in **Fig. 7b**. Even though the particle size distributions of the Inflox Fe_3O_4 and the Nanox Fe_3O_4 powders are different, there are no clear differences in their morphologies. Like in the case of the Inflox Fe_3O_4 coating, we can see clear boundaries between the slightly deformed particles and pores.

The bright field microscopy image (**Fig. 8a**) shows dark uniaxial nanograins below 100 nm in size and the column-shaped nanograins. **Figure 8b** presents a corresponding selected area for electron diffraction (SADP).

The microstructure of the conventional composite coating – Amperit 519.074 90%WC-12Co + Inflox™26FE23 10% Fe_3O_4 – is shown in Fig. 9a. There are visible areas of the dark phase, which is Inflox Fe_3O_4. The linear analysis (**Fig. 9c**) shows the presence of iron and oxygen in the microstructure coincide, which testifies to the presence of Fe_3O_4 in those areas. The counts of tungsten, on the other hand, drop nearly to zero. The microstructure of the nanostructured composite coating – Nanox™S7412 90% WC-12Co + Nanox™26FE23 Fe_3O_4 – shown in **Fig. 9b** is very similar to that of the conventional composite coating, in spite of the fact that the powders in the mixtures varied considerably in the particle size and particle size distribution. Like in the case of the conventional composite coating, the linear analysis (**Fig. 9d**) confirms the presence of the nanostructured iron oxide, Fe_3O_4. This is due to the fact that the presence and counts of iron and oxygen in the microstructure coincide.

Results of ball on disc tests

Figure 10 presents changes in the coefficient of friction for nanostructured and conventional composite coatings. There is an opposite trend in the two studied coatings. For conventional composite coating, at the

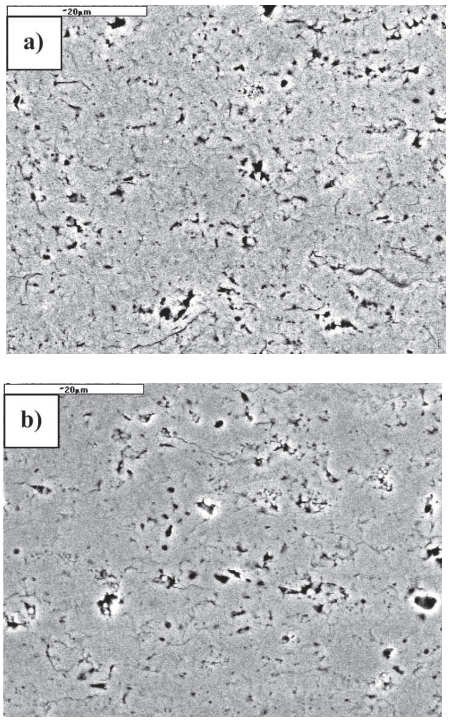

Fig. 7. Cross-sections of HVOF sprayed sprayed coating: a) Inflox 26FE23 Fe_3O_4 b) Nanox™26FE23 Fe_3O_4.
Rys. 7. Zgład metalograficzny płomieniowo natryskanej naddźwiękowo powłoki: a) Inflox 26FE23 Fe_3O_4 b) Nanox™26FE23 Fe_3O_4

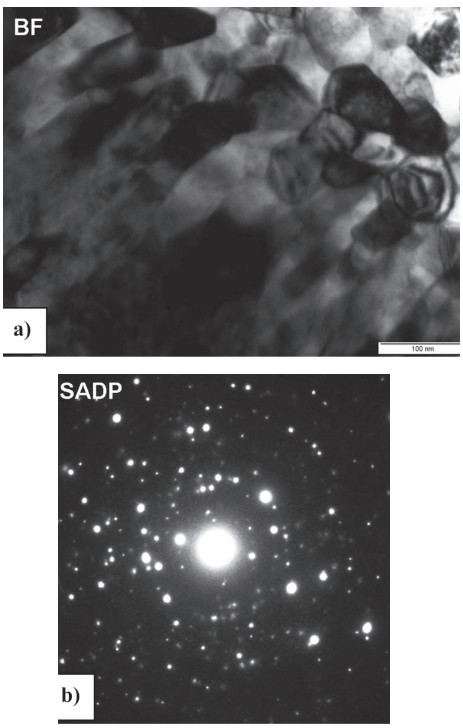

Fig. 8. Nanoparticles Fe_3O_4 in HVOF sprayed sprayed Fe_3O_4 coating : a) bright field imaging (BF), b) selected area electron diffraction (SADP)
Rys. 8. Nanocząstki Fe_3O_4 w płomieniowo natryskanej naddźwiękowo powłoce Fe_3O_4: a) obraz w jasnym polu (BF), b) dyfrakcja elektronowa (SADP)

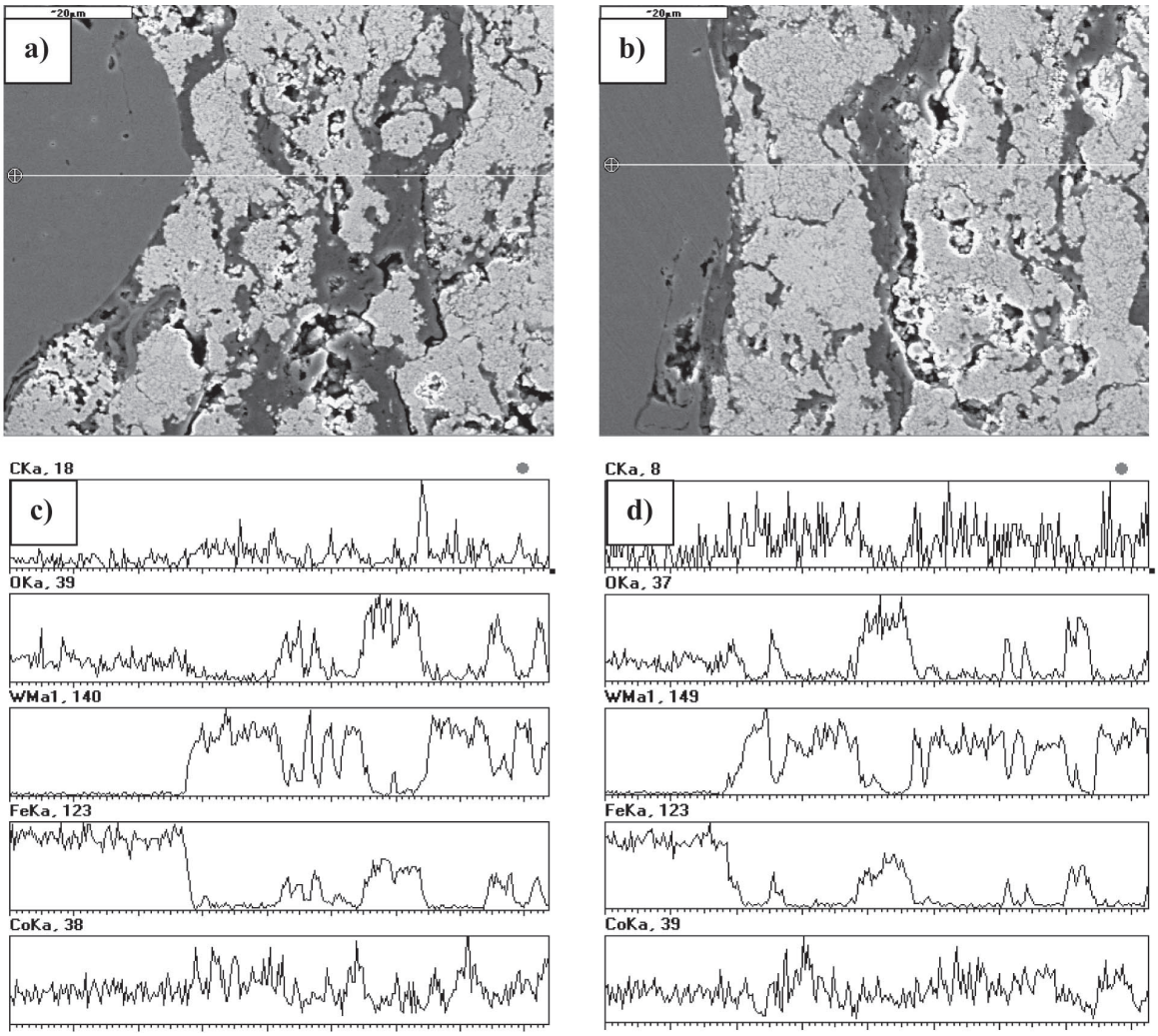

Fig. 9. Microstructure of the HVOF sprayed composite coatings: a) conventional Amperit 519.074 90%WC-12Co + Inflox™26FE23 10%Fe_3O_4, b) nanostructured Nanox™S7412 90%WC-12Co + Nanox™26FE23 10%Fe_3O_4, c) linear analysis of the coating shown in Fig. 9a, d) linear analysis of the coating shown in Fig. 9b

Rys. 9. Mikrostruktura płomieniowo natryskanej naddźwiękowo powłoki: a) konwencjonalna Amperit 519.074 90%WC-12Co + Inflox™26FE23 10%Fe_3O_4, b) nanostrukturalna Nanox™S7412 90%WC-12Co + Nanox™26FE23 10%Fe_3O_4, c) analiza liniowa powłoki pokazanej na **Rys. 9a,** d) analiza liniowa powłoki pokazanej na **Rys. 9b**

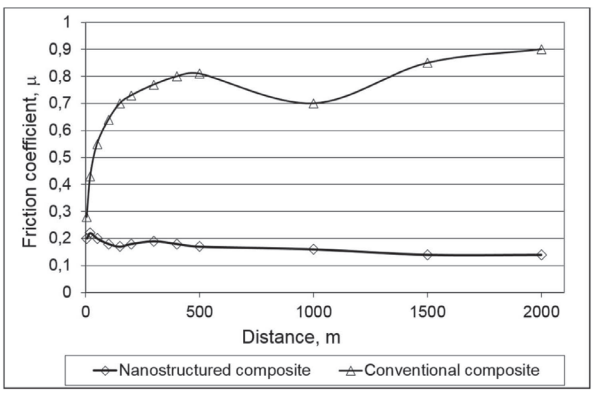

Fig. 10. The coefficient of friction for the HVOF sprayed nanostructured and conventional composite coatings

Rys. 10. Współczynnik tarcia dla płomieniowo natryskanej naddźwiękowo nanostrukturalnej i konwencjonalnej powłoki

beginning, the coefficient of friction is low, and it rises to a higher value during the running-in stage. After the first 500 m, it slightly decreases and after 1000 m reaches an almost constant slight increase. In the case of nanostructured composite coatings, the friction coefficient exhibits the steady slight decrease, and after 1500 m, it reaches an almost constant (steady-state) value of 0.15. The friction coefficient for conventional composite coatings was nearly six times higher than that obtained for the nanostructured composite coating.

The surfaces of both HVOF sprayed composite coatings after ball on disc tests are shown in **Fig. 11**. It can be inferred that these surfaces are mainly composed of tungsten carbide WC grains present in the cobalt matrix and a solid lubricant Fe_3O_4. As the result of the influence of counter sample on sprayed composite coating during ball on disc tests, the particles of Fe_3O_4

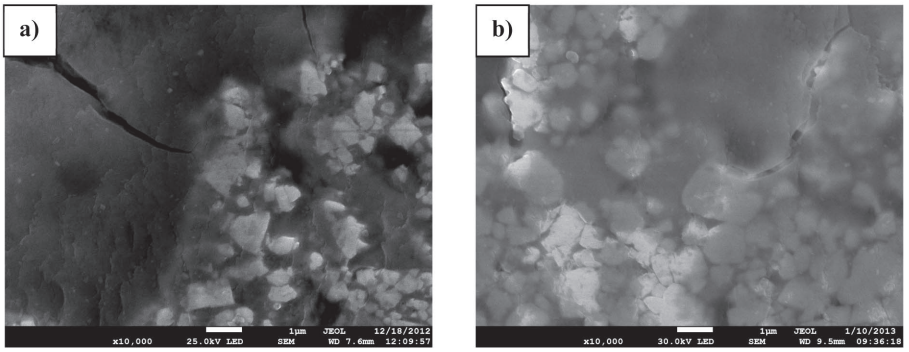

Fig. 11. Morphology of the worn surface of HVOF sprayed nanostructured and conventional composite coatings
Rys. 11. Morfologia zużytej powierzchni płomieniowo natryskanej naddźwiękowo powłoki: a) nanostrukturalnej, b) konwencjonalnej

solid lubricant fill the pores in the coating, and they are spread on the grains of the tungsten carbide and the cobalt matrix. The smooth substrate is capable of retaining an effectively spread layer of lubricant over a wide area (**Fig. 11**). Fe_3O_4 iron oxide is a material that has a layer structure along the 001 direction. As a result of the coating and 100Cr6 interaction (tests with the ball on disc type tribotester T-01), a layer of Fe_3O_4 with various thicknesses is formed. The bright WC grains covered by this layer are visible in different shades of grey in **Fig. 11**. When the 100Cr6 ball influences the larger Fe_3O_4 volumes, the cracks on its surface appear upon exceeding the yield point (**Fig. 11**). No traces of solid lubricant chipping were observed.

CONCLUSIONS

The analysed materials, which were used to produce composite coatings, considerably differed in the particle morphologies and compositions. The HVOF sprayed conventional and nanostructured Fe_3O_4 powders, Inflox Fe_3O_4, and Nanox Fe_3O_4 respectively, formed coherent coatings with small pores. There were no clear differences in their morphologies. The nanostructured Nanox Fe_3O_4 coating contained column-shaped and uniaxial Fe_3O_4 nanoparticles. When the mixtures of the conventional powders (Amperit 519.074 90%WC-12Co + Inflox™26FE23 10%Fe_3O_4) and the nanostructured powders (Nanox™S7412 90%WC-12Co + Nanox™26FE23 10%Fe_3O_4) were used, the Fe_3O_4 particles were embedded in the metal matrix composite coating, where tungsten carbide particles were the aggregate and cobalt served as the matrix. The linear analysis of the composite coatings showed that the presence of iron and oxygen in the microstructure coincide, which confirms the presence of Fe_3O_4. The counts of tungsten in these areas drop almost to zero. During sliding tests, the particles of Fe_3O_4 solid lubricant fill the pores in the coating and are spread on the grains of tungsten carbide and the cobalt matrix. Coatings sprayed from nanostructured mixture exhibited better tribological properties in comparison with coatings sprayed from the conventional mixture.

ACKNOWLEDGEMENTS

This work was funded by the Ministry of Science and Higher Education of Poland grant N503 015 32/2296.

REFERENCES

1. Burakowski T.: Aerologia. Powstanie i rozwój. ITeE – PIB, Radom 2007.
2. Bach F.W., Laarmann A., Wenz T.: Modern Surface Technology, WILEY-VCH Verlag GmbH 2006.
3. Donnet C., Erdemir A.: Historical developments and new trends in tribological and solid lubricant coatings. Surface and Coatings Technology Volume: 180-181, Complete, March 1, 2004, pp. 76–84.
4. Bolelli G., Candeli A., Lusvarghi L., Manfredini T., Denoirjean A., Valette S., Ravaux A., Meillot E.: "Hybrid" plasma spraying of NiCrAlY+Al_2O_3+h-BN composite coatings for sliding wear applications. Wear 378-379 (2017) 68–81.
5. Chunjie Huang, Wenya Li, Yingchun Xie, Marie-Pierre Planche, Hanlin Liao, Ghislain Montavon: Effect of Substrate Type on Deposition Behavior and Wear Performance of Ni-Coated Graphite/Al Composite Coatings Deposited by Cold Spraying. Journal of Materials Science & Technology 33 (2017) 338–346.
6. Jie Chen, Xiaoqin Zhao, Huidi Zhou, Jianmin Chen, Yulong An, Fengyuan Yan: Microstructure and tribological property of HVOF-sprayed adaptive NiMoAl–Cr3C2–Ag composite coating from 20°C to 800°C. Surface & Coatings Technology 258 (2014) 1183–1190.

7. Zhang G., Yuan X., Dong G.: The tribological behavior of Ni–Cu–Ag-based PVD coatings for hybrid bearings under different lubrication conditions. Tribology International 43(2010)197–201.
8. Heshmat H., Hryniewicz P., Walton II J.F., Willis J.P., Jahanmir S., DellaCorte C.: Low-friction wear-resistant coatings for high-temperature foil bearings Tribology International Volume: 38, Issue: 11–12, pp. 1059–1075.
9. Pytko S.: Podstawy tribologii i techniki smarowania. Wyd. AGH, Kraków 1989.
10. Hebda M.: Procesy tarcia, smarowania i zużywania maszyn. ITeE – PIB, Warszawa – Radom 2007.
11. Shtertser A., Muders C., Veselov S., Zlobin S., Ulianitsky V., Jiang X., Bataev V.: Computer controlled detonation spraying of WC/Co coatings containing MoS2 solid lubricant. Surface & Coatings Technology Volume: 206, Issue: 23, July 15, 2012, pp. 4763–4770.
12. Du H., Sun C., Hua W.G., Zhang Y.S. and Han Z., et al.: Fabrication and evaluation of D-gun sprayed WC–Co coating with self-lubricating property. WC–Co coating with self-lubricating property was deposited by detonation gun. Tribology Letters, 2006, Volume 23, Number 3, pp. 261–266.
13. Yuan Jianhui, Zhu Yingchun, Zheng Xuebing, Ji Heng, Yang Tao.: Fabrication and evaluation of atmospheric plasma spraying WC–Co–Cu–MoS2 composite coatings. Journal of Alloys and Compounds, Volume 509, Issue 5, 3 February 2011, pp. 2576–2581.
14. Barbezat G.: Application of thermal spraying in the automobile industry. Surface and Coatings Technology 201 (2006) 2028–2031.
15. Ford M., Fisher M.: Method for coating combustion engine cylinders by Plasma Transfered Wire Arc Thermal Spray. MSE 121 Spring 2010.
16. Borisov Y.S., Harłamow A., Sidoenko S.Ł., Adatowska E.N.: Gazotemiczeskije pokrytija iż poroszkowych mateiałow, Kijów, Naukowaja Dumka 1987.
17. Ma X.Q., DeCarmine T., Xiao T.D.: Plasma Sprayed High Lubricity Nanocomposite Coatings. International Thermal Spray Conference, Osaka 2004, pp. 812–819.
18. Fauchais P., Montavon G., Bertrand G.: From Powders to Thermally Sprayed Coatings. Journal of Thermal Spray Technology Volume: 19, Issue: 1–2, January 2010, pp. 56–80.